Amplitude calibration of a fast S-transform algorithm

Chris Bird, Kristopher Innanen, Mostafa Naghizadeh

ABSTRACT

The S-transform is a time-frequency decomposition technique with a wide range of applications in seismic signal analysis but has been under-used due to the high computational cost needed to employ it. In this paper we present a fast, non-redundant S-transform (FST). The ability of the FST to provide high fidelity estimates of the amplitudes is tested in this paper. Where the FST cannot provide accurate estimates of amplitudes, we calibrate it by normalizing the unit impulse response of the algorithm. Due to the low resolution at low frequency nature of the FST algorithm, the spectra of individual events will interfere with each other at low frequencies and limit the ability of the FST to estimate amplitudes. We discuss the limits of the calibrated S-transform to estimate amplitudes and we propose a set of standards for the fidelity of estimated amplitudes as a function of proximity in time to other events.

INTRODUCTION

Time-frequency decomposition methods provide a means to estimate the local spectrum of recorded seismic events. There are a range of time-frequency decomposition methods with applicability to seismic signal analysis (Margrave, 1997; Margrave et al., 2003). The S-transform is one such method which utilizes a Gaussian window and provides progressive resolution. The fast general Fourier family transform (FGFT) proposed by Brown et al. (2010) and implemented by Naghizadeh and Innanen (2010) provides a fast, non-redundant method of calculating the S-transform, henceforth referred to as the fast S-transform (FST). There are many motivations for performing time-frequency decomposition methods on seismic data, for instance they have been used to facilitate nonstationary seismic processing and they also provide a means to study absorption as they enable geophysicists to examine the loss of a seismic signal's highest frequencies with time. More recently, the FST has been implemented in multiple dimensions and is used as a tool for seismic interpolation (Naghizadeh and Innanen, 2010). One of our immediate problems is the estimation of target absorption from anelastic reflectivity. In order for us to estimate target absorption, we must be able to obtain high fidelity estimates of local reflection amplitudes as a function of frequency. It was our goal then, to test the ability of the FST to provide high fidelity estimates of the local spectra of seismic reflections. Where it failed to do so, we calibrated the amplitudes by normalizing the unit impulse response of the FST algorithm.

BACKGROUND

The Fourier transform (FT) does not enable us to examine the time-varying spectral content of a signal. This may be problematic because a seismic signal is often nonstationary, meaning it's frequency content changes with time. The S-transform is a time-frequency decomposition method which utilizes a Gaussian window and provides progressive resolution (Brown et al., 2010). The S-transform of a time signal $g(t)$ is defined by

Stockwell et al. (1996) and presented by Brown et al. (2010) as

$$S(\tau,\omega)=\int_{-\infty}^{\infty} g(t)\frac{|\omega|}{\sqrt{2\pi}}e^{\frac{-(\tau-t)^2\omega^2}{2}}e^{-i2\pi\omega t}dt, \tag{1}$$

where τ and ω are the time co-ordinate and frequency co-ordinate of the S-domain respectively and $\frac{|\omega|}{\sqrt{2\pi}}e^{\frac{-(\tau-t)^2\omega^2}{2}}$ is the Gaussian window. Equation (1) demonstrates how the S-transform is calculated directly from the time domain. It is possible to calculate the S-transform from the frequency domain as well. By taking the Fourier transform along the τ axis of the S-domain we generate what Brown et al. (2010) refer to as the α-domain.

$$\alpha(\omega',\omega)=\int_{-\infty}^{\infty} S(\tau,\omega)\cdot e^{-i2\pi\omega'\tau}d\tau, \tag{2}$$

where ω' is a "frequency-shift" axis generated by taking the Fourier transform along the τ axis of the S-domain. The α-domain may also be expressed as (Brown et al., 2010)

$$\alpha(\omega',\omega)=G(\omega'+\omega)\cdot W(\omega',\omega). \tag{3}$$

Here G(ω' + ω) is a matrix where each row is the Fourier transform of the signal G(ω) shifted by a frequency increment ω'. The α-domain is generated by multiplying this matrix by the Fourier transform of the window functions W(ω',ω). Once the α-domain is constructed, the S-domain is obtained by performing an inverse Fourier transform along the ω'-axis of the α-domain. The equation for calculating the S-domain from the α-domain is given in Brown et al. (2010) as

$$S(\tau,\omega)=\int_{-\infty}^{\infty} \alpha(\omega',\omega)\cdot e^{-i2\pi\omega'\tau}d\omega'. \tag{4}$$

Figure 1 shows how the S-domain may be constructed from the α-domain with an example time signal. Figure 1(a) shows a time signal which is a sum of two harmonics of 10 Hz and 50 Hz. The Fourier transform of this signal is shown in Figure 1(b). G(ω' + ω) is a matrix such that every row is the Fourier transform of the original signal shifted by ω', this is shown in Figure 1(c). W(ω',ω), the FT of the window functions is shown in Figure 1(d). The α-domain, (e), is achieved by multiplying every row of G(ω' + ω) with every row of W(ω',ω). Finally, taking the inverse fast Fourier transform (IFFT) along ω', expressed by (4), yields the S-domain of the original signal (Figure 1f) . Notice that the S-domain shows that the signal is stationary and contains only two frequencies, 10 Hz and 50 Hz, as expected.

As presented in Brown et al. (2010) and implemented by Naghizadeh and Innanen (2010) the ST can be calculated non-redundantly by segmenting in the α-domain, with high frequencies being coarsely sampled and low frequencies being finely sampled. The α -domain is divided up into segments, with large segments for high frequencies and small segments for low frequencies. For each of these segments only one frequency at the centre

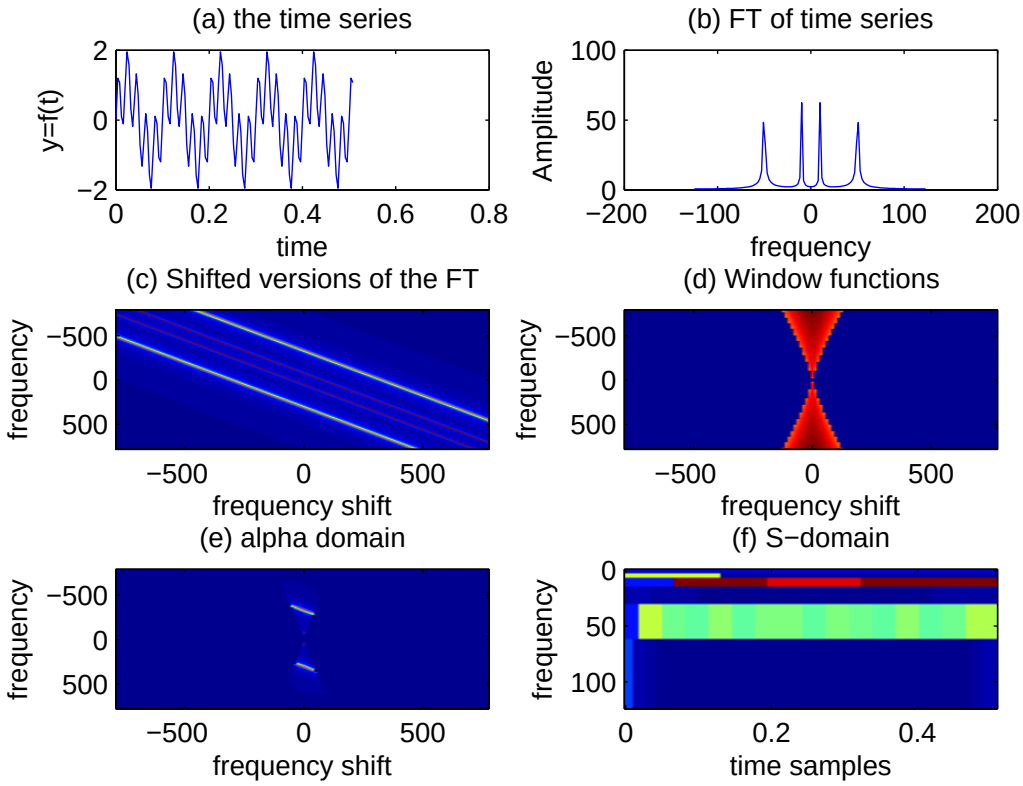

FIG. 1. Construction of S-domain from α domain. (a) is an example time signal which is the sum of two harmonics of 10 Hz and 50 Hz. (b) is the Fourier transform of the time signal. (c) is the matrix $G(\omega' + \omega)$ which is populated by shifted versions of (b). (d) is the matrix $W(\omega', \omega)$ which is the Fourier transform of the window functions. (e) is the α-domain obtained by mutliplying $G(\omega' + \omega)$ with $W(\omega', \omega)$. (f) is the S-domain.

of the segment is sampled and these values are used for all frequencies enclosed by the segment. Finally, to generate the S-transform an inverse fast Fourier transform (IFFT) is applied to each segment. The IFFT of each segment populate their corresponding frequency range in the S-domain for the entire τ axis. Thus, since at larger frequencies we have larger segments we gain time resolution but we lose frequency resolution. For low frequencies we gain high frequency resolution but have poor time resolution. This method of segmenting the α-domain makes the calculation of the ST fast and non-redundant and yields the fast S-transform (FST).

Figure 2 shows a unit impulse (Figure 2a) and it's corresponding S-domain generated by the FST (Figure 2b). Figure 2(c) shows a profile through the S-domain at the time sample of the unit impulse, hence Figure 2(c) shows the unit impulse response (UIR) of the FST. The Fourier spectrum of a unit impulse is well known to be a constant value at unity for all frequencies. By looking at Figure 2(c) it can be seen that the spectrum of the unit impulse is not a constant value but rather increases with a "stair-case" trend. The goal of this paper is to calibrate the amplitude spectrum of the FST by removing the fast transform algorithm footprint, as observed in Figure 2, by correcting it's unit impulse response to be a constant value at unity.

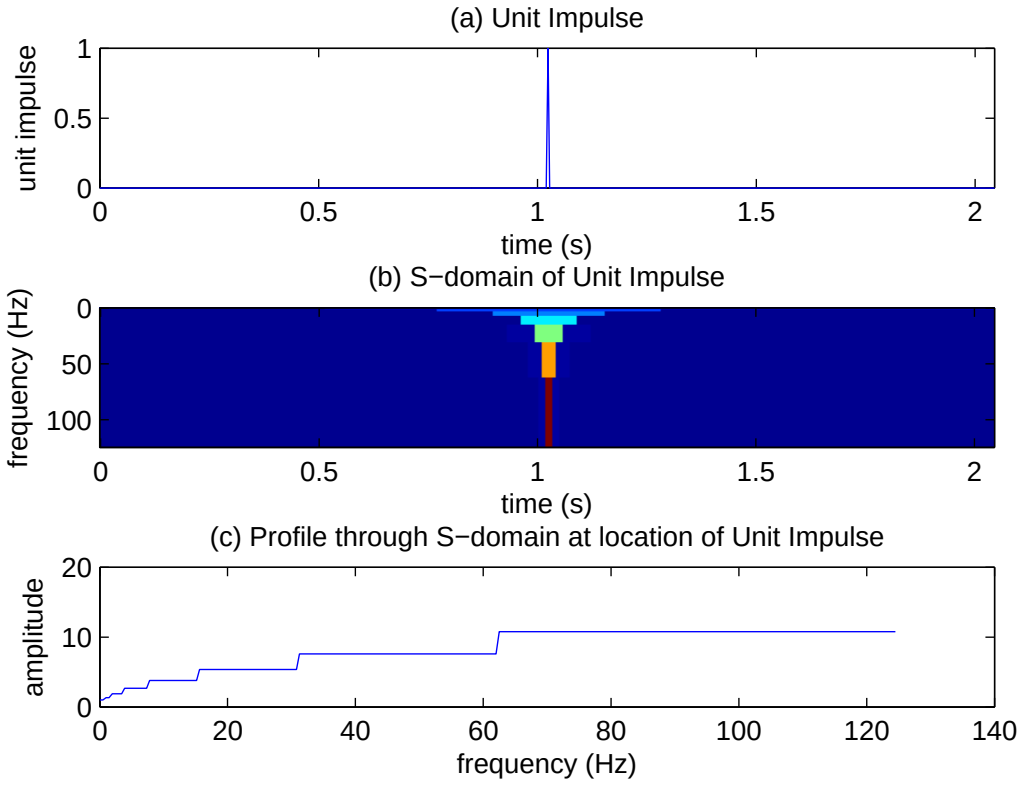

FIG. 2. UIR of FST before any corrections. (a) is a unit impulse input into the FST. (b) is it's S-domain and (c) is a frequency profile through the S-domain at the time sample of the unit impulse.

AMPLITUDE CALIBRATION OF THE FST ALGORITHM

In order to characterize the footprint of the FST algorithm, a series of tests were performed. In the first test, unit impulses at the centre of empty vectors of varying sizes were input into the FST algorithm and the UIR was observed for all of these vectors. For example, in Figure 2 the unit impulse is at the centre of a 512 point vector. The "stair-case" increase of amplitude with frequency, as shown in Figure 2, was observed for all vector sizes. Investigating further, it was noticed that in the original FST algorithm there was a scaling factor of $1/\sqrt{N}$ applied with the IFFT of the individual segments in the α-domain, where N is the number of samples in the segment. This scaling was corrected to the proper scaling of $1/N$. After implementing this correction the same tests were performed again to observe the UIR. Figure 3 shows the UIR of the FST after this correction, Figure 3(a) shows the unit impulse input into the FST, Figure 3(b) is the S-domain of the unit impulse and Figure 3(c) shows the amplitudes picked from the S-domain. It is clear from Figure 3 that the "stair-case" increase of amplitude with frequency has been eliminated and the spectrum is closer to a constant value. However, the amplitude of the UIR drops to 0.95 at roughly 5 Hz and then stays relatively constant. This is close to the desired UIR but there is still some residual algorithm footprint which needs to be addressed.

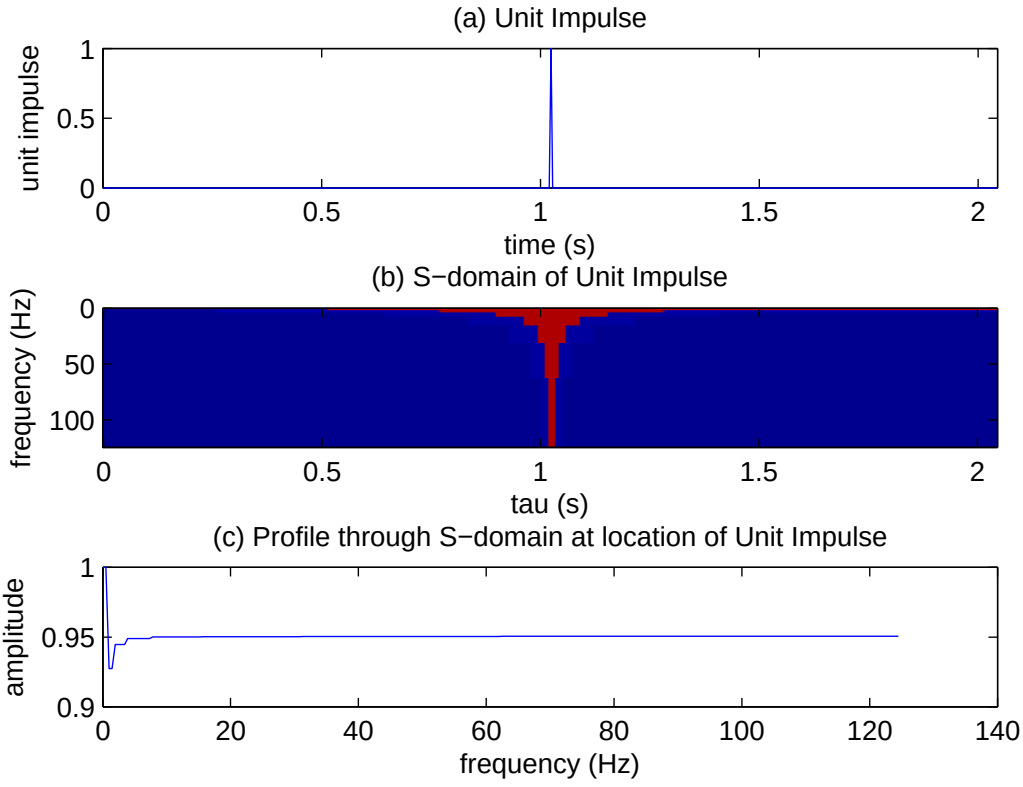

FIG. 3. UIR after 1/N scaling correction. (a) is a unit impulse input into the FST. (b) is it's S-domain and (c) is a frequency profile through the S-domain at the time sample of the unit impulse.

Another test performed was to vary the position of a unit impulse within an empty vector and observe the S-domain of the unit impulse. A number of these unit impulses

were input into the FST and the S-domain was examined to determine if the UIR was dependent on position of the impulse in time. Figure 4 shows two separate unit impulses at the 50th and 350th sample within a 512 point vector, their S-domains, and their profiles through the S-domain. The distinctly different S-domain profiles of these two unit impulses shows that there is a dependence of the UIR on the location of the unit impulse in time.

In order to correct the UIR for the dependence on position of the impulse and all other residual footprint, a code was developed which calculates and implements the corrections needed to make the spectrum of a unit impulse, at any location in time, a constant at unity. The corrections are stored in a matrix and then the matrix is multiplied with the S-domain. This matrix will hereafter be referred to as the FST spectrum fidelity correction matrix (SFCM). For every N-point signal there is a corresponding NxN point S-domain and SFCM. For a given input signal, the SFCM is found by first determining the UIR at every location in time. Then for each of these UIR's a set of N scaling coeficients is produced by determining the multipliers needed to scale the UIR to a constant value at unity. This is carried out by dividing 1 by the UIR at all frequencies. Hence, the j_{th} row of the SFCM contains the scaling coefficients that need to be multiplied with the S-domain spectrum at the j_{th} time sample. The SFCM corrects the dependence of the UIR on position in time and it also takes care of all other residual algorithm footprint. With this correction matrix applied to the S-domain, a unit impulse input into the FST algorithm at any location will yield the desired constant value. Figure 5 Shows the S-domain for a unit impulse with the SFCM applied and it's profile in the S-domain. As can be seen, the UIR is as desired.

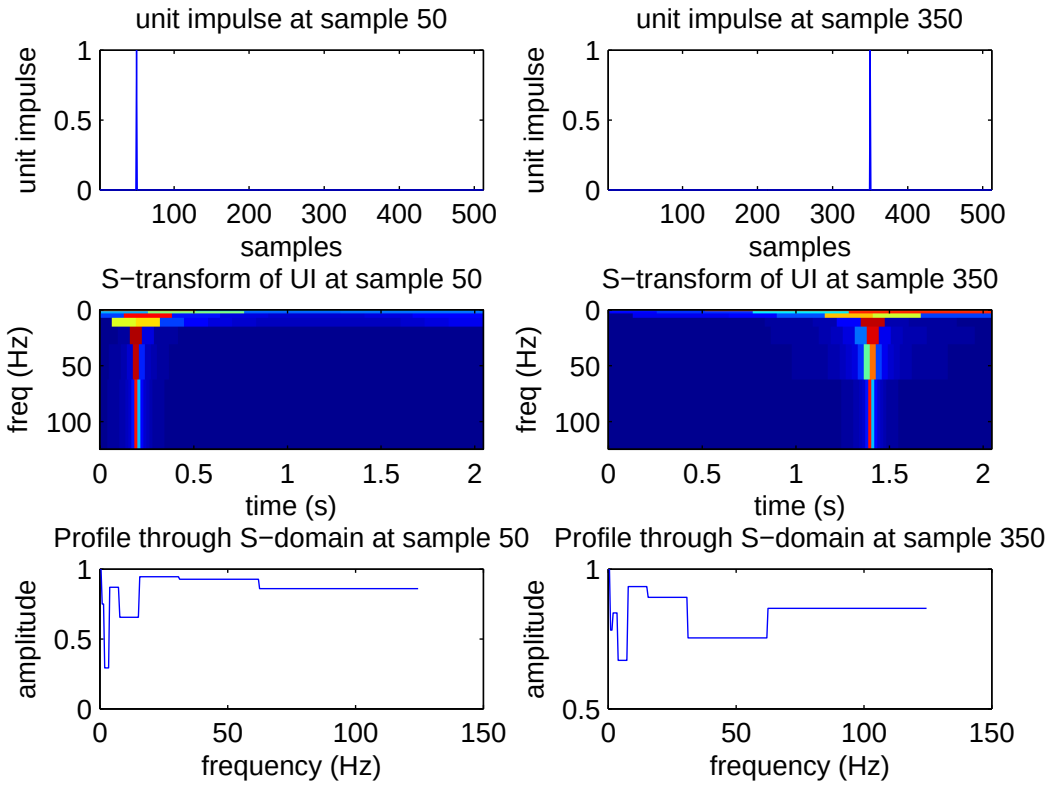

FIG. 4. Dependence of the position of the unit impulse on the UIR of the FST algorithm. The top two panels show two unit impulses which were input into the FST at 50th and 350th time sample respectively. The middle two panels show their respective S-domains and the bottom two panels show their frequency profiles through the S-domain.

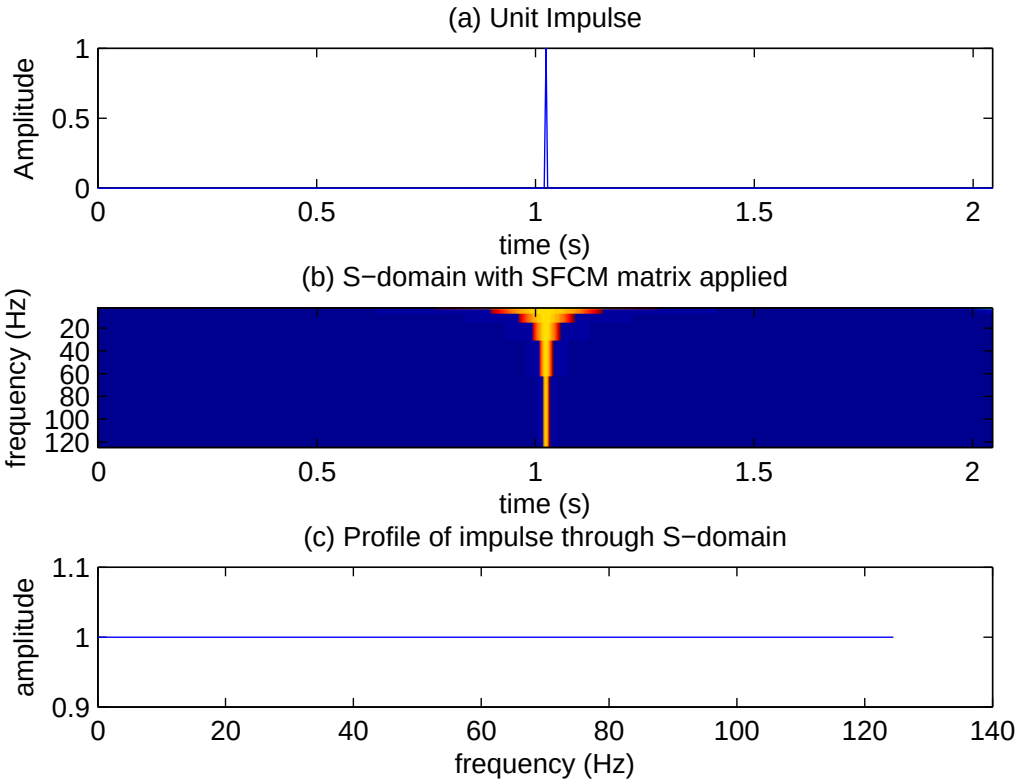

FIG. 5. Unit Impulse Response of FST after calibration. In (a) we have a unit impulse in time. In (b) we have the calibrated S-transform of the unit impulse and in (c) we see the frequency profile of the unit impulse through the S-domain

LIMITS OF THE AMPLITUDE CALIBRATION

The spectrum generated by the FST algorithm has low time resolution at low frequencies, therefore, even with the SFCM applied, the spectrum of individual events will interfere with each other at low frequencies even when the events are separated in time. Also, the range of frequencies at which spectrums of individual events interfere with each other is greater the more proximal events are to each other. Because of this, it is important to develop a set of standards which define the fidelity of an events' spectrum as a function of it's proximity to other events. Two unit impulses were input into the FST at opposite ends of an otherwise empty vector and then the S-domain was observed to determine the lowest frequency at which the spectrum of the individual impulses did not interfere with each other(henceforth called the cut-off frequency). Then each unit impulse was moved one sample closer in time and again the S-domain was examined for the cut-off frequency. This procedure continued until the separation of the impulses approached zero. Figure 6 through Figure 9 shows the S-domain of two unit impulses and their S-domain profiles for time separations of 240 samples, 180 samples, 90 samples and 20 samples respectively. Figure 6(a) shows the S-domain of two unit impulses which are 240 samples apart, as can be seen from their profiles(Figure 6(b) and 6(c)) the individual spectra of these two events only interfere with each other at very low frequencies. However, as the separation between

the impulses decreases(Figure 8, 9, and 10) it can be seen that the individual spectra are interfering with each other at higher and higher frequencies. To quantify the cutoff frequency a code was written which determines the lowest frequency at which the amplitude of the unit impulses spectra is within 8 percent of unity. Then the cutoff frequency was plotted against the number of samples separating the unit impulses and is shown as the blue line in figure 10. As expected, the more proximal the impulses are to each other the higher the cutoff frequency becomes. The green line in Figure 10 is an exponential decay curve which was least squares fit to the cutoff frequency curve. Because there is so much variance to the cut-off frequency curve(Figure 10), a qualitative study of the cutoff frequency as a function of impulse separation was performed and is shown in figure 11. There still appears to be an inverse exponential relationship but now the plot is easier to interpret. Based on the results of Figure 11, I suggest that it is safe to trust frequencies above 8 Hz for events which are separated by more than 34 samples from other events.

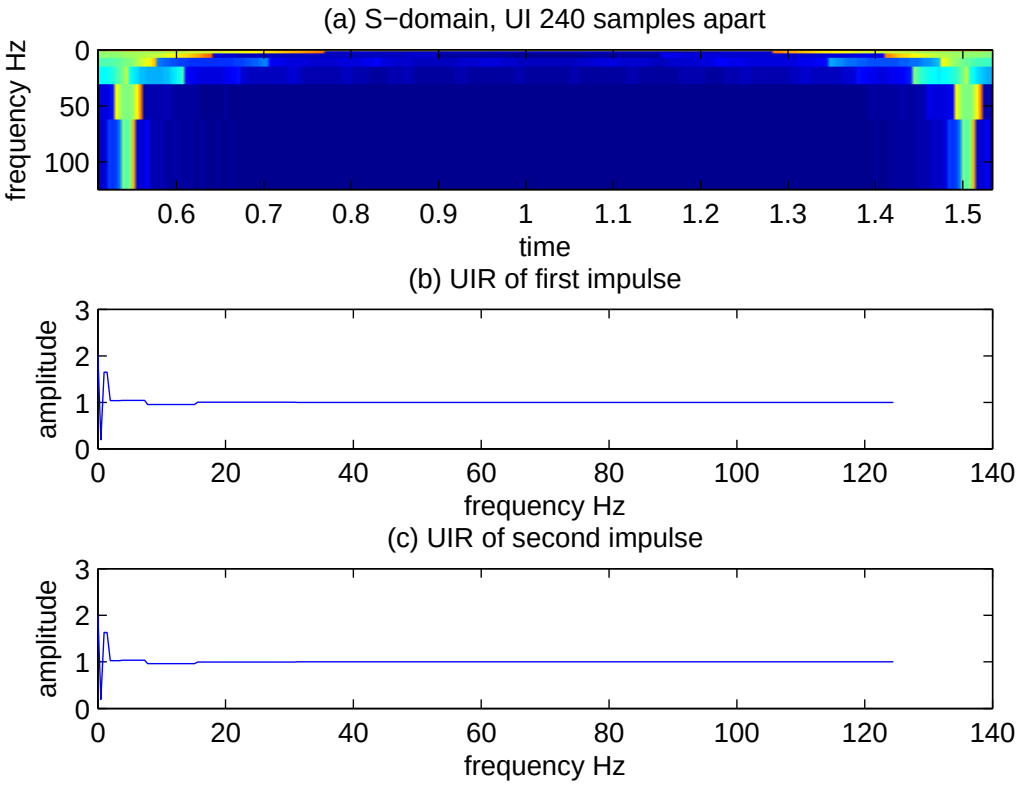

FIG. 6. S-domain of two unit impulses 240 samples apart. (a) shows the S-domain of the two unit impulses input into the FST simultaneously. (b) and (c) show their respective frequency profiles through the S-domain.

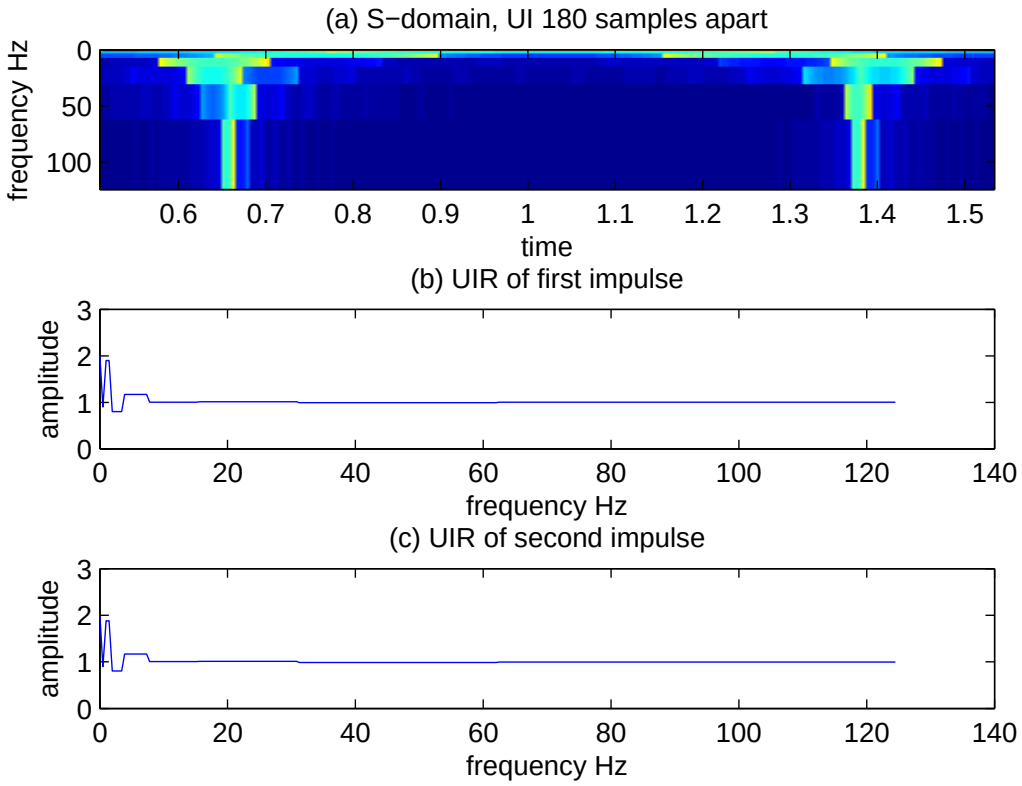

FIG. 7. S-domain of two unit impulses 180 samples apart. (a) shows the S-domain of the two unit impulses input into the FST simultaneously. (b) and (c) show their respective frequency profiles through the S-domain.

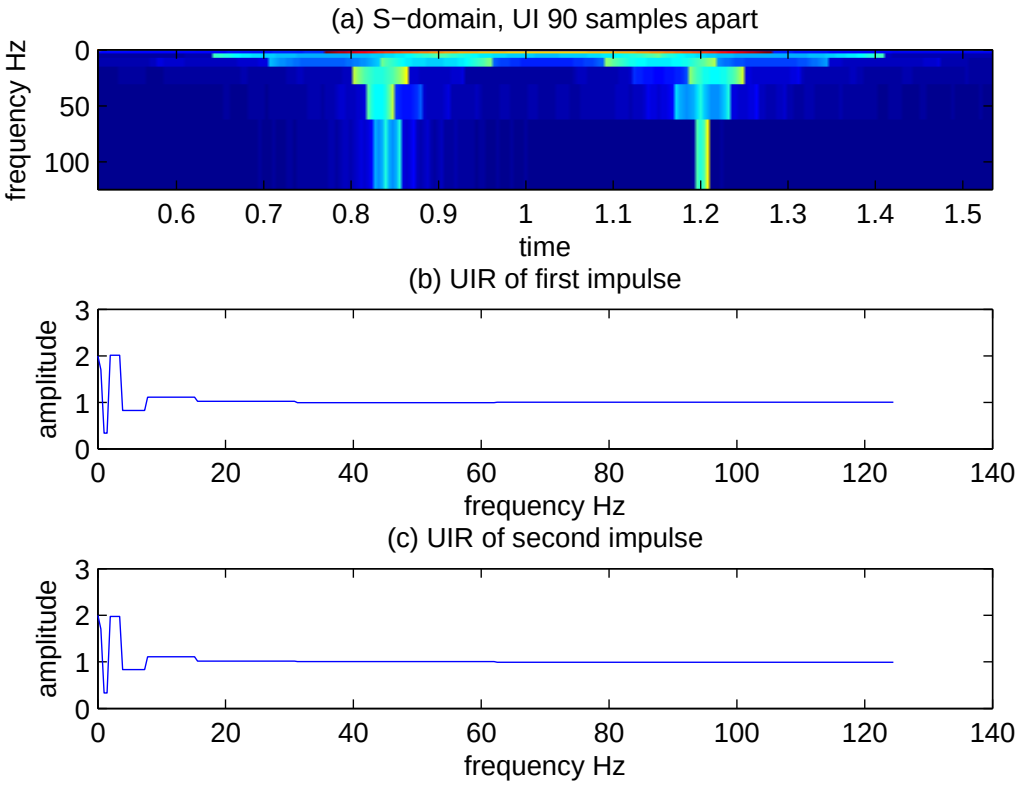

FIG. 8. S-domain of two unit impulses 90 samples apart. (a) shows the S-domain of the two unit impulses input into the FST simultaneously. (b) and (c) show their respective frequency profiles through the S-domain.

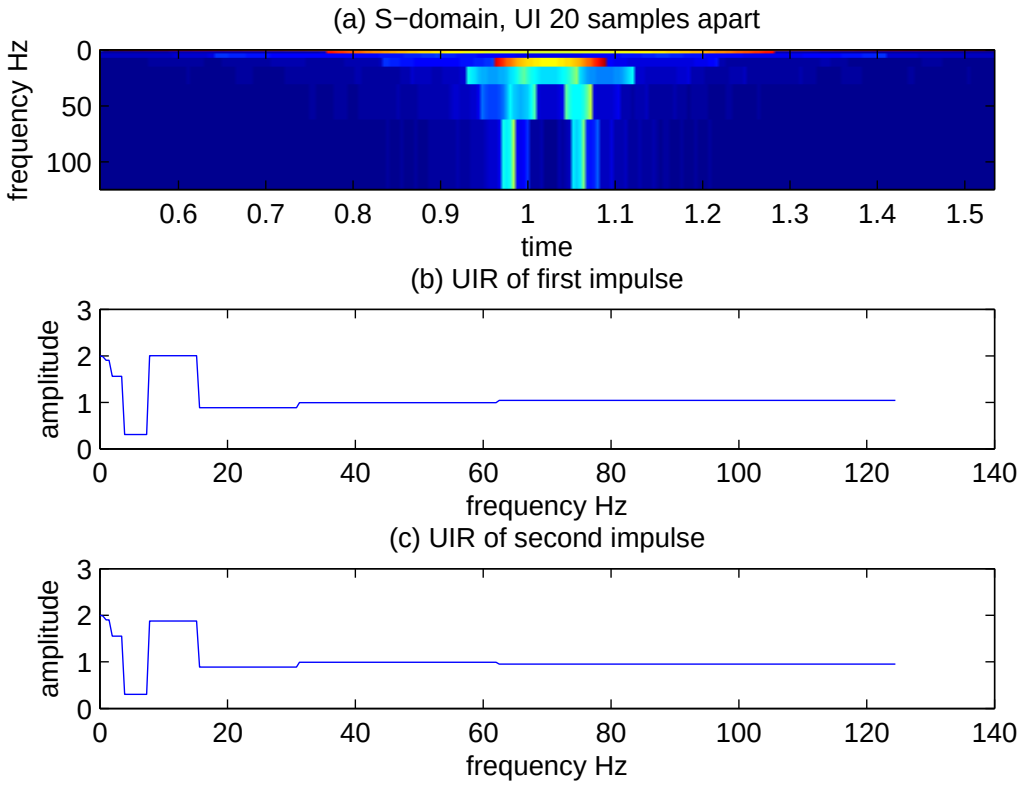

FIG. 9. S-domain of two unit impulses 20 samples apart. (a) shows the S-domain of the two unit impulses input into the FST simultaneously. (b) and (c) show their respective frequency profiles through the S-domain.

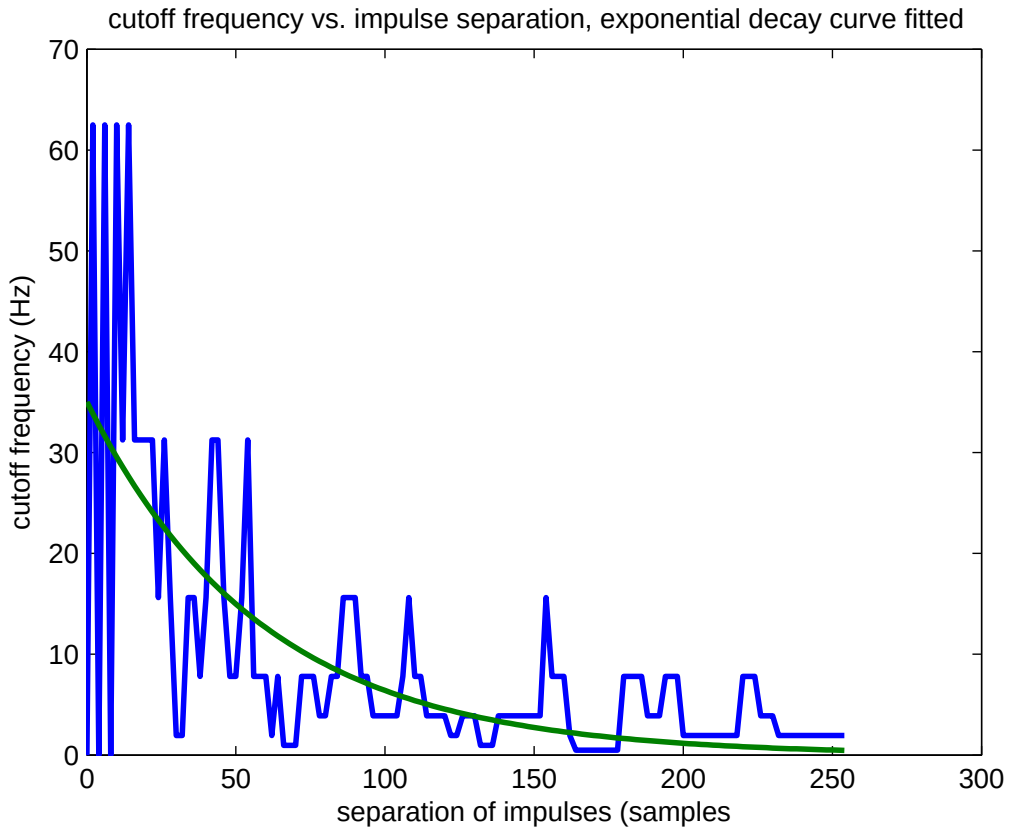

FIG. 10. cutoff frequency vs. impulse separation, Quantitative approach. The green curve is an exponential decay which was fit to the data.

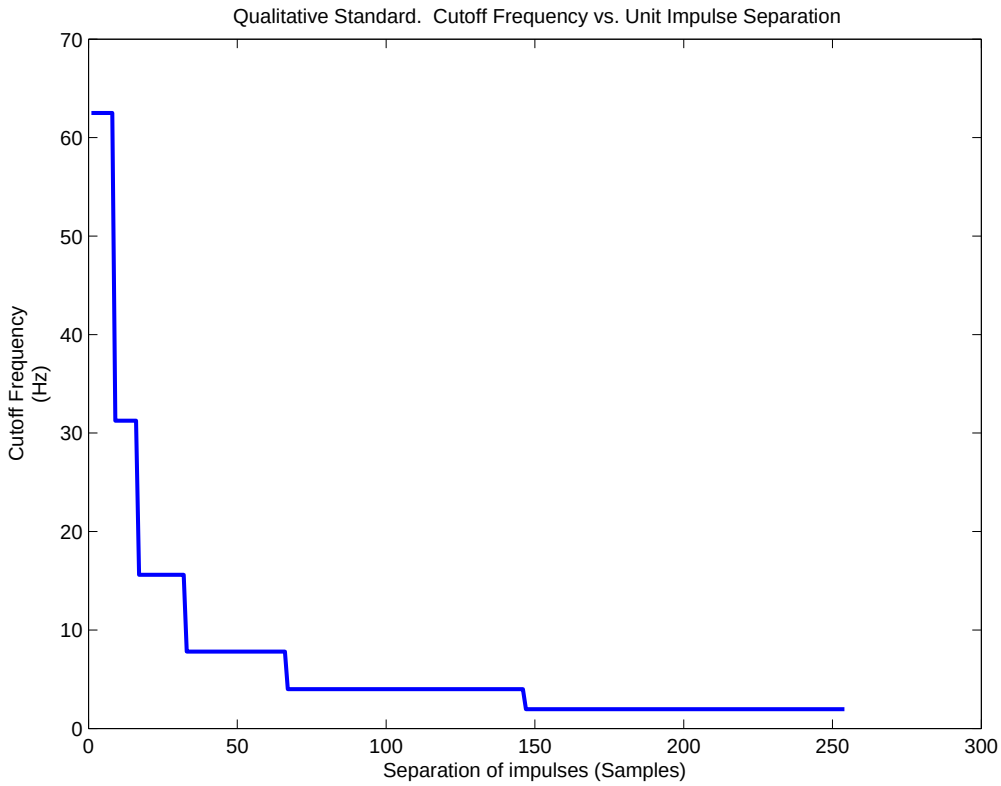

FIG. 11. cutoff frequency vs. impulse separation, Qualitative approach

CONCLUSIONS

The FST, proposed by Brown et al. (2010) and implemented by Naghizadeh and Innanen (2010) provides a fast, non-redundant method of time-frequency decomposition with a wide range of applicability to seismic signal analysis. The amplitude spectrum of the FST algorithm was calibrated by normalizing the unit impulse response. This calibration was carried out by calculating and implementing the spectrum fidelity calibration matrix which is multiplied directly with the S-domain. Also, limits on the usefulness of the amplitude calibration, due to the low time resolution at low frequencies nature of the algorithm, were discussed and a set of standards for determining the validity of the spectra of individual events as a function of proximity to other events was established. One of our immediate uses for this calibrated fast S-transform is the estimation of target absorption parameters from anelastic reflectivity (Bird et al., 2010). The authors conclude that the calibrated FST, provides a useful seismic signal analysis tool.

REFERENCES

Bird, C., Naghizadeh, M., and Innanen, K., 2010, Amplitude calibration of a fast S-transform: CREWES Sponsor's Meeting 2010, , No. 4, 1–12.

Brown, R. A., Lauzon, M. L., and Frayne, R., 2010, A general description of linear time-frequency transforms and formulation of a fast, invertible transform that samples the continuous S-transform spectrum nonredundantly: IEEE Transactions on Signal Processing, **58**, No. 1, 281–290.

Margrave, G. F., 1997, Theory of nonstationary linear filtering in the Fourier domain with application to time-variant filtering: Geophysics, **63**, 244.

Margrave, G. F., Henley, D., Lamoureux, M. P., Iliescu, V., and Grossman, J., 2003, Gabor deconvolution revisited, *in* Proc. 76th Ann. Mtg., Dallas TX, Soc. Expl. Geophys.

Naghizadeh, M., and Innanen, K., 2010, Fast generalized Fourier interpolation of nonstationary seismic data: CREWES Sponsor's Meeting 2010.

Stockwell, R. G., Mansinha, L., and Lowe, R., 1996, Localization of the complex spectrum: The S transform: IEEE Trans. Signal Process, **44**, No. 4, 2957–2962.